Proceedings of The Institute of Acoustics

MODELS OF TURBULENT NOISE SOURCES IN THE VOCAL TRACT

Christine H. Shadle

Institute of Sound and Vibration Research, University of Southampton, Southampton SO9 5NH England

INTRODUCTION

Fricative consonants are produced when the vocal tract is constricted somewhere along its length enough so that air passing through the constriction produces a hissing sound (see Fig. 1). In English, the unvoiced fricatives are /f,θ,s,š/ (as in "*f*in, *th*in, sin, *sh*in"). For some of these fricatives it appears that sound is also generated by the air exiting the constriction and striking an obstacle downstream of the constriction, such as the teeth in /s,š/ or the lips in /f/. Fant [1], Flanagan and Ishizaka [2] and others, have modeled fricatives by adding one or more plane-wave pressure sources to a one-dimensional acoustic tube model. Whether this has a physical justification, and the limitations of such models, have been explored very little.

This paper presents theoretical calculations and results of experiments with mechanical models designed to investigate source models for fricatives. The questions of interest are: is the behavior influenced by the surrounding duct? and, how well can we predict this behavior with a one-dimensional transmission-line model? Mechanical models were used because the articulatory and aerodynamic parameters could be controlled more exactly than in humans. They consisted of two idealized configurations: a cylindrical constriction in a circular duct, and the same constriction with a semicircular downstream obstacle. The simple shapes made the development of theoretical models relatively straightforward. The presence of the obstacle was shown by preliminary experiments to be acoustically significant. In addition, the obstacle used was similar in shape and position to the teeth, and thus seemed likely to play an acoustically similar role.

THEORY

Jet noise has been investigated extensively. The theory of jet noise is based on the work of Lighthill [3], who described the monopole, dipole, and quadrupole sources, and discussed their use in modeling turbulence. Dipole sources occur along rigid boundaries, which exert an alternating force on the fluid; quadrupole sources exist in free jets. Although the strength of the quadrupole sources increases with flowrate at a much higher rate than that of dipoles (the sound power is proportional to v^8 rather than v^6), quadrupole

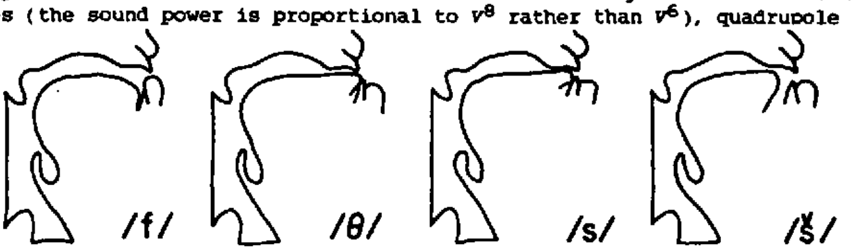

Fig. 1. Diagram of the midsagittal cross-section of the vocal tract during the production of the fricatives /f,θ,s,š/, as in "*f*in, *th*in, sin, *sh*in."

sources are much less efficient radiators of sound. Thus at the low Mach numbers typical of speech, dipole sources can be expected to dominate.

On this basis, the most reasonable source models for the obstacle and no-obstacle cases considered here appear to be the following. The sound generated by the jet is represented by a distribution of weak quadrupole sources downstream of the constriction; the obstacle case model has, in addition, stronger dipole sources located at the obstacle, to represent the sound generated as the jet impinges on it. The orientation of the flow dipoles is assumed to be longitudinal (i.e. parallel to both the jet and the duct axes) since the plane surface of the obstacle can only support forces in the longitudinal direction. As a first approximation, we neglect the quadrupole sources relative to the dipole sources for the obstacle case.

Preliminary results [4] with the mechanical models support these source models. First, the sound produced is of much greater intensity when the obstacle is present. Second, when the constriction is mounted flush with a plane baffle, and the obstacle is suspended in free space downstream of the constriction, the directivity pattern measured is distinctly dipole-like, with minima at 90° to the jet axis. Third, in this setup, the far-field sound pressure should be the sum of the sound produced by the dipoles at the obstacle and that produced by their reflection in the baffle. Interference effects are therefore predicted, at specific frequencies dependent on the angle of the observer and the distance between obstacle and baffle. The measured spectra contained minima at the predicted frequencies, further supporting the dipole model.

A dipole source can be modeled as two out-of-phase simple sources a distance d apart, each generating a volume-velocity U. The total dipole strength is then $S = Ud$. The predicted far-field sound pressure due to a dipole and its reflection in a baffle is

$$p_o\ (r,\theta,\omega) = \frac{\omega^2 \rho}{4\pi c}\, S \left[\frac{\cos\,\theta}{r}\ e^{-jkr} - \frac{\cos\,\phi}{R}\ e^{-jkR}\right] \qquad (1)$$

where $\omega = 2\pi f = 2\pi$ *(frequency)*, c = speed of sound, $k = \omega/c$, and r,R,θ,ϕ are defined in Fig. 2. Dividing both sides of Eqn. (1) by S, we obtain an

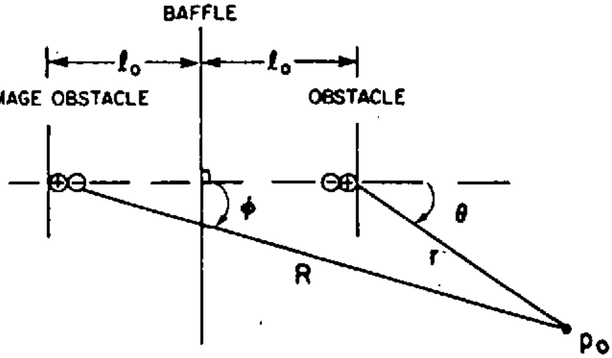

Fig. 2. Schematic of dipole reflected in baffle, defining r,R,θ,ϕ,l_o.

expression for the ratio $\hat{p}_o(r,\theta,\omega)/S(\omega)$. We can think of this ratio as a transfer function that specifies the effect of the baffle on the source, and therefore derive an estimate of the source function, $\hat{S}$, by inverse filtering the measured pressure $p_o(r,\theta,\omega)$:

$$\hat{S} = \frac{p_o\ (r,\theta,\omega)}{\hat{p}_o\ (r,\theta,\omega)/S(\omega)} \tag{2}$$

We now wish to find an equivalent source p_s in terms of $\hat{S}$. p_s will be used to model sound generation inside the tube, where only plane waves propagate (for frequencies less than the first cutoff frequency, which is about 8 kHz). If we make the assumption that all of the sound radiated by the flow dipoles excites longitudinal modes of the tube, we can approximate the spherical sources comprising the dipole by plane-wave sources of the same strength U. The distance d separating them becomes a transmission-line section of (small) length d, which is represented by an acoustic mass of value $\rho d/A$, where A is the cross-sectional area of the duct. It is then straightforward to derive the pressure drop across the circuit, which is then the strength of the equivalent pressure source:

$$\hat{p}_S\ (\omega) = j\left(\frac{\omega\rho}{A}\right)\widehat{Ud} = j\left(\frac{\omega\rho}{A}\right)\hat{S} \tag{3}$$

We now have an expression for the sound source generated by the obstacle in a tube that depends only on the sound measured when the obstacle is in free space. We would like to see if this is a good model, and whether the source as so defined remains the same when the obstacle is contained within the duct. To do so, the experiments schematized in Fig. 3 were devised. The transfer functions T_3 and T_{12} were derived using transmission-line representations of the duct for the different positions of constriction and obstacle. The derived transfer functions were multiplied by the source functions, derived from experiment as described above, to produce a predicted output for each configur-

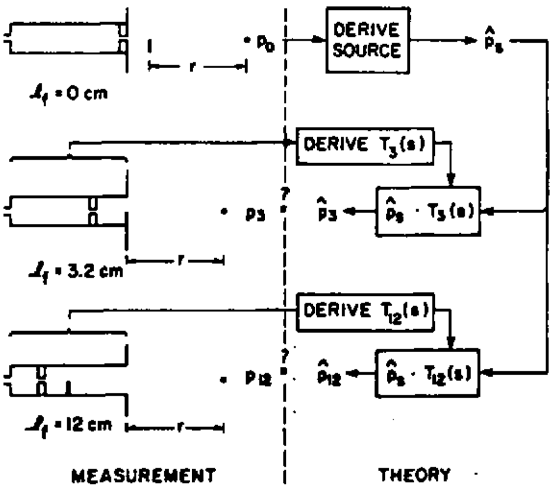

Fig. 3. Diagram of the predictions and comparisons to be made for the obstacle case.

ation, which was compared to sound spectra measured for the actual configurations. The procedures for the mechanical model experiments will be described in the next section. A few words are in order here about the method of deriving the transfer functions.

These transfer functions are derived by simulating the tubes with a pressure source at the location of the obstacle, using an iterative solution of the plane-wave propagation equations [5,6]. Losses due to radiation, heat conduction, viscosity, and flow resistance of the constriction were included in the model. The effects of the various model parameters can be summarized as follows. The natural frequencies of the entire tract are excited by the source; because of the relatively small area of the constriction, the front and back cavities are nearly decoupled, and the natural frequencies are approximately equal to the quarter-wavelength resonances of the front cavity and the half-wavelength resonances of the back cavity. Radiation loss at the mouth of the tube lowers all of the "front-cavity" resonances and increases their bandwidths; this effect is more pronounced for a greater mouth area proportionate to the front-cavity volume. In addition, the pressure source in the front cavity excites anti-resonances, near zero Hz and at frequencies approximately equal to the half-wavelength resonances of the back cavity and of the portion of the front cavity between the source and the constriction. Thus, the "back-cavity" resonances and anti-resonances effectively cancel each other. The remaining anti-resonances are not subject to radiation loss; viscosity and heat conduction cause some damping at low frequencies, shifting the first anti-resonance up in frequency slightly. Higher anti-resonances appear in the predicted spectrum as relatively sharp minima, with frequencies very sensitive to the distance between the obstacle and the constriction. Comparison of these predictions to the measured spectra will demonstrate how well the pressure source model works, and whether there is evidence of interaction of the source with the tube.

METHOD

Figure 4 shows the experimental setup used. Air passes from the tank through a flowmeter, past a pressure manometer, through a muffler that provides acoustic isolation, and finally into a tube which has the configuration under consideration. The sound generated is picked up by a microphone and fed into an HP spectrum analyzer, which computes an RMS-averaged spectrum (for a 10 kHz frequency range, sixteen 12.5 msec windowed spectra are averaged together).

For the experiments reported on here, the constriction is always a 1 cm long aluminum cylindrical plug with an axial circular hole 3 mm in diameter. It is positioned in a 17 cm long, 2.5 cm diameter plastic tube, either 0, 3, or 12 cm from the mouth. The obstacle is a semicircular piece of aluminum of the same radius as the tube, and 2 mm long. When used, it is 3 cm downstream of the constriction. Finally, flowrates between 160 and 420 cc/sec were used, which covers the range used by people producing fricatives. This results in a flow velocity through the constriction of between Mach 0.06 and 0.20.

RESULTS

Figure 5 shows the estimates of p_s derived from the sound pressure measured for a 0 cm front cavity at four flow rates. The p_s curves are noisy and have a peak around 6 kHz. The small-scale perturbations are random in nature and

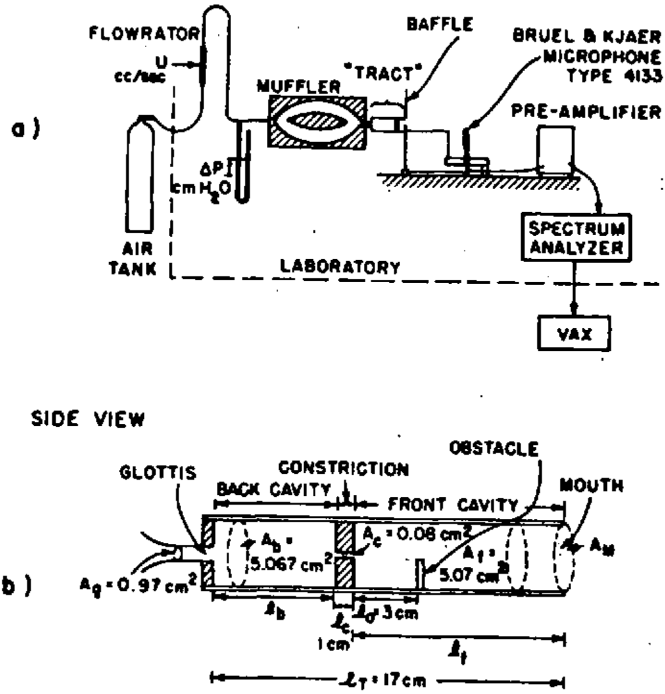

Fig. 4. a) Diagram of the setup for the mechanical model experiments. The tract, whose outer wall is a cylindrical tube, is shown in cross section in b) of the figure.

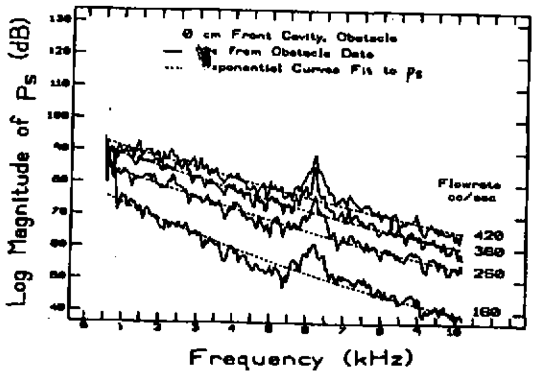

Fig. 5. a) Far-field sound pressure p_o at four flowrates, with regressed room noise. b) Equivalent pressure source p_s derived from p_o. For both cases, l_f = 0 cm, obstacle is 3 cm downstream of constriction.

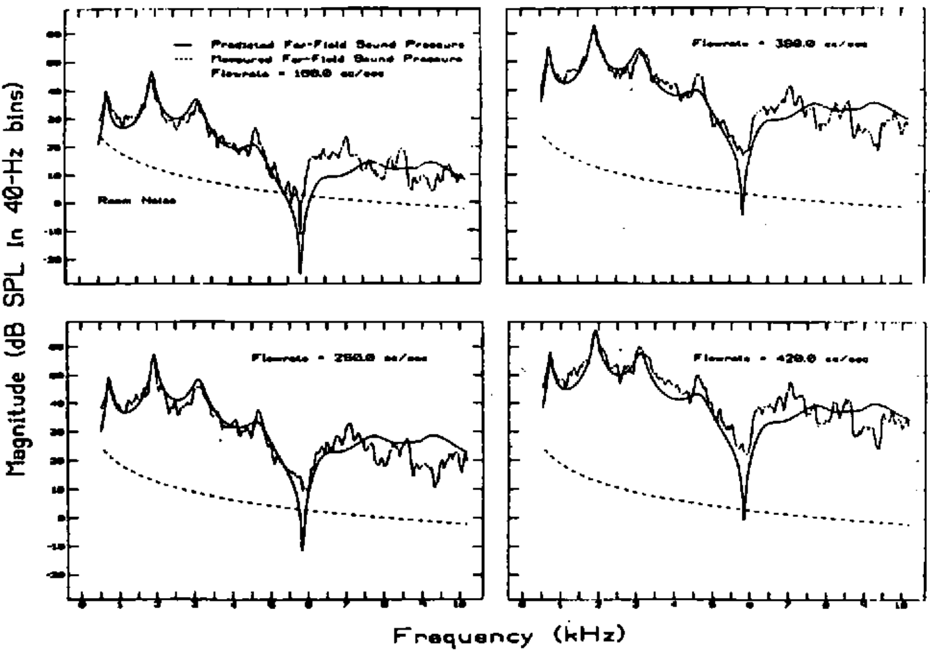

Fig. 6. Far-field sound pressures for front cavity length l_f = 12 cm, obstacle 9 cm from mouth; measured, p_{12}, versus predicted, $\hat{p}_{12}$, at four flowrates.

tend to smooth out as more averages are taken; individual wiggles are unimportant. The peak at 6 kHz indicates that the interference effect is not quite as severe as predicted. This is indicative of slight problems with our source model, but for the comparisons we are about to make, it is unimportant and makes it more difficult to compare. Thus, these curves were regressed, excluding the peak, resulting in the dashed lines shown, and the regressed curves were used as the source functions.

Figure 6 shows the predicted and measured curves for a front cavity of 12 cm at the same four flow rates. The fits are very good with regard to both the spectral shape and absolute level. At 5.7 kHz, the frequency of the predicted zero, the data exhibit only a modest "dip". This is due in part to the smearing effect of the window, but is also evidence of a less than perfect source model. If, for instance, the source were modeled not as a single dipole but as a set of dipoles spatially distributed by even 1 mm along the tube axis, then the depth of the predicted minimum would also be more modest. Finally, the slight mismatch of bandwidths is due mainly to the approximation made in the model of the radiation out the open end of the duct. Overall, the fit is quite good, indicating that there is very little interaction between the sound source and the filtering action of the tube. Results for l_f = 3.2 cm are similar.

To check for the possibility of interaction in a different way, we looked at

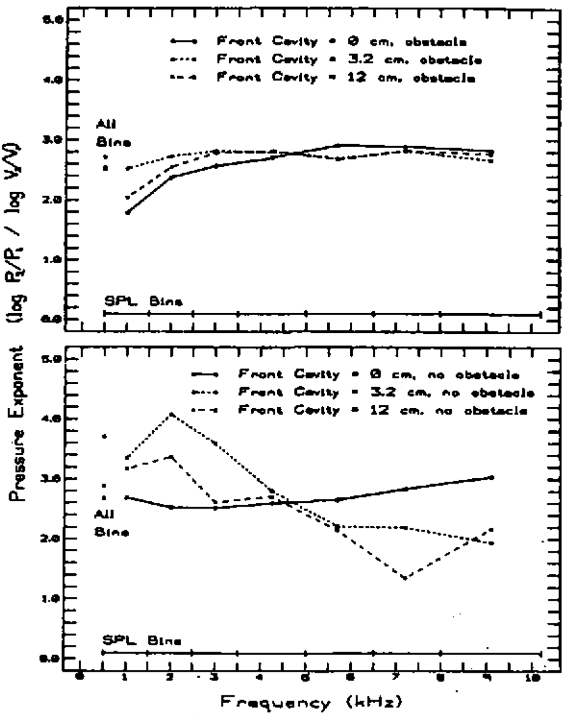

Fig. 7. Pressure exponents for the three obstacle (top) and no-obstacle (bottom) configurations. Each point represents the change in sound pressure with respect to flow velocity over the frequency range indicated by the markings on the line labeled "SPL Bins". The points labeled "All Bins" are computed over the entire range of 500 to 10200 Hz.

the relationship between sound pressure and flow velocity for the three configurations. The intensity of the sound generated by monopole, dipole and quadrupole sources depend on, respectively, the fourth, sixth and eighth powers of the flow velocity. Therefore, one way of checking for source-tract interaction is to see if the power laws differ as the tract — the length of the front cavity — changes. In Fig. 7 we see that the pressure exponents are nearly the same for all three front cavity lengths, indicating that there is no source-tract interaction for these configurations. Its average value across all frequencies of roughly 2.5 is slightly less than the 3.0 we would expect for flow dipoles, and much less than the value of 4.0 that would be expected for quadrupoles. It thus appears that the assumptions on which the source model were based were valid.

Because of the extreme low amplitude of the sound generated for the no-obstacle case, particularly when the constriction was at the mouth of the tube, it was not possible to derive a source spectrum from data and use it to test the source model as in the obstacle case. The no-obstacle case was tested for interaction effects in two ways, however. First, the predicted resonances were subtracted from each spectrum, leaving behind a residue spectrum consisting of the anti-resonances excited by the source and the source spectrum itself. These residue spectra should be identical regardless of front-cavity length, if the same sound is generated in each case. In fact, they differed by as much as 10 dB. Computation of the pressure exponents yielded a similar result, which can be seen in Fig. 7: unlike for the obstacle case, they differed for the two front-cavity lengths, and also were on average of higher value, closer to that expected of a quadrupole source. A likely explanation is that sound is generated along the walls of the tube; if they are not included in the determination of the source model, there will appear to be source-tract "interaction."

CONCLUSION

Two mechanical models were studied that are simplified, idealized representations of configurations actually occurring in fricative sounds. The obstacle case, that model in which a jet strikes an obstacle in a tube, produced a radiated spectrum that is well-modeled by measurements of sound produced by the obstacle in free space used together with a linear plane-wave model of the tube system. Thus for this configuration an independent source-filter model is valid, with a pressure source at the obstacle. For the no-obstacle case, it was shown that there is interaction if the source is considered to be determined by the jet alone; it appears that sound generation occurs along the walls of the tube, and thus a more realistic model would include the walls as a source-determining factor.

In related work [4] it has been demonstrated that the obstacle case is a good model of the fricatives /s,š/. It appears that other fricatives fall between the obstacle and no-obstacle cases: there is significant sound generation along the walls of the tract or at obstacles that are not at right angles to the flow. For such fricatives, more complex source models will be necessary.

[This work was supported by NIH-NINCDS.]

REFERENCES

[1] Fant, G. Acoustic Theory of Speech Production. Mouton, The Hague (1960).

[2] Flanagan, J. and K. Ishizaka "Automatic Generation of Voiceless Excitation in a Vocal Cord-Vocal Tract Speech Synthesizer," IEEE-ASSP 24 no. 2, 163-170 (1976).

[3] Lighthill, M.J. "On Sound Generated Aerodynamically: II. Turbulence as a Source of Sound," Proc. Roy.Soc. A222, 1 (1954).

[4] Shadle, C.H. "The Acoustics of Fricative Consonants," unpub. Ph.D. thesis, Dept. of Elect. Engr. Comp. Sci., M.I.T.; released as Tech. Rept. 506, Resch. Lab. of Elect., M.I.T. (1985).

[5] Henke, W. "Dynamic Articulatory Model of Speech Production Using Computer Simulation," App. B, Unpub. Ph.D. thesis, Dept. of Elect. Engr. Comp. Sci., M.I.T. (1966).

[6] Hosein, P. "Computer Simulation of a Model for the Vocal Tract," Unpub. B.S. thesis, Dept. of Elect. Engr. Comp. Sci., M.I.T. (1983).

Proceedings of The Institute of Acoustics

A STUDY OF SOUND TRANSMISSION LOSS IN A RECTANGULAR ATTENNUATOR LINED WITH A PARABOLIC WALL CONDUCTANCE

F.B. Shenoda (1) and H. Selim (2)

(1) National Institute for Standards , Dokki , Cairo
(2) IBM Cairo Scientific Center , Cairo , Egypt

ABSTRACT

The sound attenuation in a free path rectangular duct of constant crossectional area was theoretically studied for the case of a parabolic change of wall conductance. The solution of the obtained Bessel differential equation consists of a combination of modified Hankel functions of the order 1/3.

The parabolic change of the wall conductance can be realized by means of a homogenious sound absorbing flow resistance together with a slit which changes parabolically along the length of the attenuator.

The attenuator characteristics at a certain frequency were found to depend only on the duct length (L) and an attenuator characteristic area (A_c):

$$A_c = \frac{S\sqrt{L}}{g_o\, b}$$

; where S = actual attenuator cross-sectional area,
g_o = normalized wall conductance at a distance of 1 cm from attenuator input.
b = slit width at the end of the duct

When this attenuator is introduced as a termination to a hard duct, an input reflection coeff. of the order of 0.1 and a transmission loss of the order of 30 dB were calculated for a freq. > 100 HZ , L= 150 cm and A_c = 1000 cm^2.

Experimental results were in fair agreement with the theoretical results.

INTRODUCTION

Sound attenuation in ducts lined with local, constant and homogenious wall admittance has been extensievly studied [1-3]. As a result of these studies, a number of graphs has been published. These graphs deliver the attenuation for a given complex wall admittance of the lining, the duct height and sound frequency [2,3,4,6]. However, sound attenuators having a constant complex wall admittance lining can only be easily designed if narrow frequency band operation is desired. Also Ingard et Al [7] and Kurze [4] studied the sound propagation in a duct with different wall lining. Heins et Al [8] studied the sound propagation in a duct with two different values of wall impedance.

In the present work the sound attenuation as well as the input wave impedance in one dimensional rectangular duct lined with a parabolically increasing real wall admittance are theoretically studied, and experimentally verified for the case of this duct being inserted bet. two hard ducts of equal cross-sectional area. Such a duct can be used as a sound attenuator as well as an anechoic termination with free path.

A STUDY OF SOUND TRANSMISSION LOSS IN A RECTANGULAR ATTENUATOR LINED WITH A PARABOLIC WALL CONDUCTANCE

ATTENUATOR DUCT LINED WITH PARABOLIC INCREASING WALL CONDUCTANCE

In the following analysis, plane wave propagation will be assumed by limiting the largest cross dimension to approximately half the minimum wave-length. In this case the wave equation for the velocity potential u(x) is given by [3].

$$\frac{d^2 u(x)}{dx^2} + (K_o^2 - i \frac{K_o}{h} . \rho C . G) u(x) = o \qquad (1)$$

where K_o = the wave number = $2 \pi / \lambda$

G = the local wall conductance

= particle velocity normal to the lined wall / (sound pressure)

h = the effective height of the duct

= $\frac{\text{duct cross-sectional area (S)}}{\text{absorbent width along the prephiry (a)}}$

ρC = characteristic air impedance

i = $\sqrt{-1}$

Assuming the wall conductance to be a function of x, a closed form solution of eqn. (1) will be derived for the case of the parabolic variation of the wall conductance according to the relation

$$G(x) = G_o \sqrt{x} \qquad (2)$$

where G_o [1/ Rayl. cm $^{\frac{1}{2}}$] is the wall conductance at a distance 1 cm from the inlet of the duct.

This can be realized by means of lining the duct with a material having constant conductance, whereby the parabolic change is attained by means of a parabolic slit of maximum width 'b' at the end of the attenuator of length 'L'. In this case the effective height is given by

$$h_{eff} = \frac{S}{b} \sqrt{\frac{L}{x}} \qquad (3)$$

According to Cremer [3] the condition for plane wave propagation will hold if

$$\rho C\, G_o << K_o \quad h_{eff} << \frac{1}{\rho C\, G_o} \qquad (4)$$

Introducing eqn. (2,3) in eqn.(1) gives

$$\frac{d^2 u(x)}{dx^2} + (K_o^2 - i \frac{K_o}{A_c} x) u(x) = 0 \qquad (5)$$

where $A_c = \frac{S \sqrt{L}}{\rho C \; G_o \, b}$ = attenuator characteristic area [cm^2].

Using the following transformation

$$z = - K_o A_c + i x$$

eqn. (4) takes the form

$$\frac{d^2 u(z)}{dz^2} + \frac{K_o}{A_c} z \; u(z) = 0 \qquad (6)$$

Further, by means of the transformation

$$u(z) = \sqrt{z} \cdot Q(T) \quad \text{and } T = \frac{2}{3}\sqrt{\frac{K_o}{A_c}} \cdot z^{3/2}$$

equation (6) finally becomes

$$\frac{d^2 Q}{dT^2} + \frac{1}{T} \cdot \frac{dQ}{dT} + \left(1 - \frac{(1/3)^2}{T^2} \right) \cdot Q(T) = 0$$

This is a Bessel differential equation of order one-third and has the closed form solution

$$Q(T) = C_1 \; H^{(1)}_{1/3} \; (T) + C_2 \; H^{(2)}_{1/3} \; (T) \qquad (7)$$

where C_1 and C_2 are arbitrary integration constants and $H^{(1),(2)}_{1/3}(T)$ are Hankel functions first and second kind [9] of the complex argument T and the order 1/3. The 2 functions are triple-valued functions of T, with a branch-point at the origin . The product, however, of the two multiple valued functions $T^{1/3}$ and $H^{(1),(2)}_{1/3}(T)$ is the single valued function $h_{1,2}(z)$, which represents the modified Hankel functions of the order one third.
These functions are related to each other by the equations

$$T^{1/3} \; H^{(1)} \; (T) = h_1 \left(z \sqrt[3]{\frac{K_o}{A_c}} \right)$$

$$T^{1/3} \; H^{(2)} \; (T) = h_2 \left(z \sqrt[3]{\frac{K_o}{A_c}} \right)$$

Accordingly, the complete solution of the differential equation (5) is given by

$$u(z) = \sqrt{z} \cdot Q(T) = \sqrt{z} \cdot T^{-1/3} \left(C_1 \; h_1 \; (az) + C_2 \; h_2 \; (az) \right)$$

The solution represents the incident as well as the reflected waves. For harmonic time dependence of the sound field, the sound pressure P(x) and the particlle velocity are then given by

$$P(x) = - i \omega \rho \, u(x) = d_1 \; (C_1 h_1 \; (az) + C_2 \; h_2 \; (az)) \qquad (8)$$

$$v(x) = \frac{du(x)}{dx} = d_2 \; (C_1 \; h_1' \; (az) + C_2 \; h_2' \; (az)) \qquad (9)$$

where h_1' and h_2' are the derivatives of h_1 and h_2 respectively and

$$a = \sqrt[3]{\frac{k_o}{A_c}} \quad , \quad d_1 = - i \omega \rho \left(\frac{9 A_c}{4 k_o} \right)^{1/6}$$

$$d_2 = i \; (9 k_o \; / \; 4 A_c \;)^{1/6}$$

Such an attenuator, when used for noise attenuation in air ducts, is usually inserted between 2 hard ducts of equal cross-section.

Considering this configuration we use the boundary conditions at the input of the attenuator duct, namely the continuity of sound pressure and sound flux, to determine the constants C_1 and C_2 of eqn. (8,9).

On the other hand, the boundary conditions at the end of the attenuator deliver the expressions for the reflection coefficient (r) and the normalized wave impedance $\left(\frac{Z_o}{\rho C}\right)$

$$r = \frac{B_1 N_1 - B_2 S_1}{B_2 S_2 - B_1 N_2} \tag{10}$$

and

$$\frac{Z_o}{\rho C} = \frac{1+r}{1-r} \tag{11}$$

also the sound transmission loss ΔL can be calculated and is given by

$$\Delta L = 20 \log \left| \frac{\rho C d_2 M}{h_1 (az_L) (S_1 + rS_2) - h_2 (az_L) (N_1 + rN_2)} \right| \tag{12}$$

where

$$B_1 = d_1 h_2 (az_L) - \rho C d_2 h_2' (az_L)$$

$$B_2 = d_1 h_1 (az_L) - \rho C d_2 h_1' (az_L)$$

$$S_1 = \frac{\rho C d_2 M}{h_1 (az_o)} + \frac{h_2 (az_o)}{h_1 (az_o)} \cdot N_1$$

$$S_2 = \frac{\rho C d_2 M}{h_1 (az_o)} + \frac{h_2 (az_o)}{h_1 (az_o)} \cdot N_2$$

$$N_1 = \rho C d_2 h_1' (az_o) - d_1 h_1 (az_o)$$

$$N_2 = \rho C d_2 h_1' (az_o) + d_1 h_1 (az_o)$$

$$M = h_1 (az_o) h_2' (az_o) - h_2 (az_o) h_1' (az_o)$$
$$= -i\, 1.457495$$

$$z_o = z_{x=o} = -K_o A_c$$
$$z_L = z_{x=L} = -K_o A_c + i L$$

INFINITE LINED DUCT

The sound transmission loss of the limiting case of an attenuator of infinite length will be calculated . This will also give the sound transmission loss of many practical configurations, by which the reflected energy at the end of the attenuator is negligible [10] due to the high sound attenuation of the incident wave . In this case only the incident sound wave propagates down the attenuator. This means that the constant $C_2 = 0$ in eqn. (8,9) and accordingly the normalized wave impedance of the input of the infinite attenuator is given by

A STUDY OF SOUND TRANSMISSION LOSS IN A RECTANGULAR ATTENUATOR LINED WITH A PARABOLIC WALL CONDUCTANCE

$$\frac{Z_{o\infty}}{\rho C} = \frac{P(o)}{v(0)} \frac{1}{\rho C} = -(K_o^2 A_c)^{1/3} \frac{h_1(az_o)}{h_1'(az_o)}$$

$$= -F \cdot \frac{h_1(-F^2)}{h_1'(-F^2)} \quad (13)$$

and F = a frequency parameter

$$= (K_o^2 A_c)^{1/3}$$

The reflection coefficient r_o at the inlet of the infitire attenuator is given by

$$r_\infty = \frac{\frac{Z_{o\infty}}{\rho C} - 1}{\frac{Z_{o\infty}}{\rho C} + 1} \quad (14)$$

Using the results of the infinite attenuator a limiting value for the transmission loss (ΔL^*) can be calculated . ΔL^* gives the transmission loss of an attenuator of finite length which fullfills the condition of negligible reflected energy at its end. In this case

$$\Delta L^* = 20 \log \frac{P(x=o)}{P(x=L)} = 20 \log \frac{h_1(az_o)}{h_1(az_L)}$$

THEORETICAL RESULTS

Some representative results were calculated for different duct lengths of 100, 150 and 200 cm . It was found that for $A_c > 500$, the condition of eqn. (4) is valid in the medium frequency range between 100 and 1000 Hz for wide range of duct heights and lengths.

Fig (1a) depicts the change of ΔL as a function of frequency for different duct lengths at constant attenuator characteristic area A_c of 1000 cm^2. Fig. (1b) shows the corresponding change of the input reflection coefficient (r) .

Fig.2 shows ΔL and r for constant duct length of 100cm and for different values of A_c, namely 500, 1000, and 5000cm^2.

The change of the real and imaginary parts of the normalized input impedance are given in fig.3 for L=100cm , and A_c=1000cm^2.

As seen from eqn.(13,14), the reflection coefficient for the limiting case 'r' (case of neglilible reflected sound energy at attenuator end) is only a function of the frequency parameter 'F'. This gives the unique representation of the reflection coefficient of fig.4 for arbitrary attenuator parameters.

A STUDY OF SOUND TRANSMISSION LOSS IN A RECTANGULAR ATTENUATOR LINED WITH A PARABOLIC WALL CONDUCTANCE

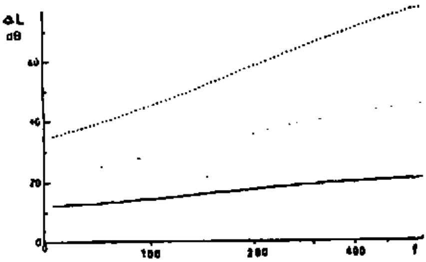

Fig.1a

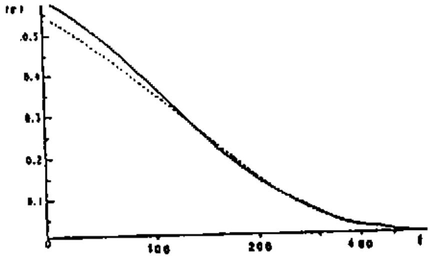

Fig.1b

A_C = 1000cm² and L = 100 —— , 200 .... ,and 300cm ---

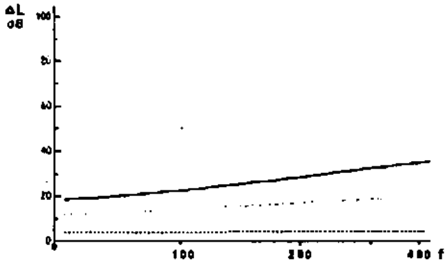

Fig.2a

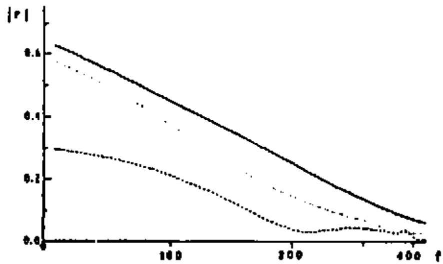

Fig.2b

L = 100cm , and A_C = 500 —— , 1000 .... , and 5000cm² ---

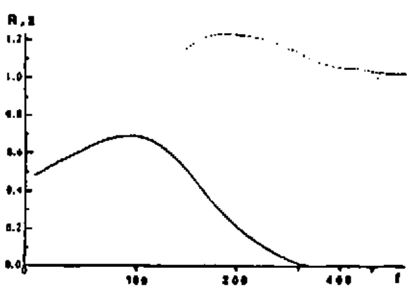

Fig.3

($R_Z/\rho C$) .... , and ($X_Z/\rho C$) ——

for L = 100cm , and A_C = 1000cm²

A STUDY OF SOUND TRANSMISSION LOSS IN A RECTANGULAR ATTENUATOR LINED WITH A PARABOLIC WALL CONDUCTANCE

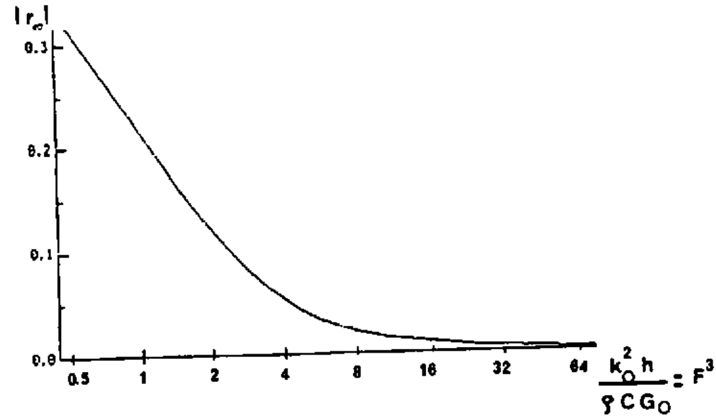

Fig.4

Normalized r_∞

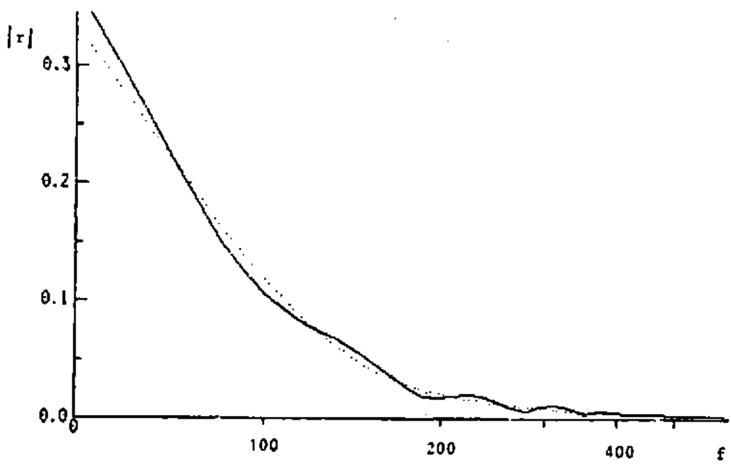

Fig.5

r_∞ .... , and r ——

for L=200cm , and A_c=5000cm²

Fig. 5 shows a comparison of this limiting value r_∞ and the corresponding value for A_c = 5000 cm^2 and L = 200 cm . As seen from fig.5, the exact calculated and the limiting values are comparable. This is due to the relatively large value of L and the corresponding small reflected energy at the end of the attenuator.

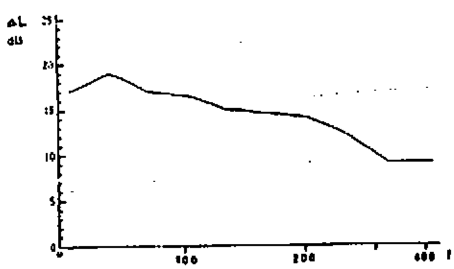

Fig.6a

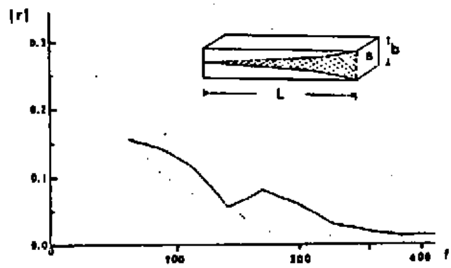

Fig.6b

Measured —— against Calculated ...

for L=200cm , and A_c=5000cm²

ATTENUATOR REALIZATION AND EXPERIMENTAL RESULTS

For testing the calculated reflection coefficient and the calculated sound transmission loss a rectangular duct was designed having a length of 200 cm and a cross-sectional area of 16x10 cm^2 . One of its larger sides was lined such that a value of A_c = 5000 was attained [10].

The parabolic change of the wall conductance can be realized by means of a homogenious sound absorbing flow resistance together with a slit which changes parabolically along the length of the attenuator. By the experimental implementation of this slit a variable perforation area having the same dependence on x and a perforation ratioof 35% was used.

In order to prevent the sound propagation in the lining parallel to the duct, thin partitions in the lining were used at a distance of 20 cm apart. The comparison of the experimental and theoretical results are depicted in fig.6 .

The decrease of the measured ΔL in deviation to the calculated values can be explained by the unavoidablly added imaginary part of the wall impedance due to the vibrating air mass inside the lining. The value of this added part obviously increases with increasing the frequency. As seen from fig.6b, the measured and calculated values of the reflection coefficient are in fair agreement.

A STUDY OF SOUND TRANSMISSION LOSS IN A RECTANGULAR ATTENUATOR LINED WITH A PARABOLIC WALL CONDUCTANCE

CONCLUSION

The gradual parabolic increase of the wall conductance of an attenuator is shown to give low values of input reflection coefficient at relatively high values of sound transmission loss.

This attenuator, which can be easily realized, allows a wide frequency band operations. This is due to the frequency independence of its lining.

Having a free path and a constant cross-sectional area this attenuator can have many applications; for example as an attenuator for air-conditioning ducts, as an unechoic termination for machine testing with non zero flow by the in-duct method, or as an exhaust silencer.

REFRENCES

[1] L.J. Sivian, 'Sound propagation in ducts lined with absorbing materials', J.A.S.A., vol. 9, 135, (1937).

[2] P.M.Morse, 'The transmission of sound inside pipes', J.A.S.A., vol. 11, 205, (1939).

[3] L. Cremer, 'Theorie der Luftscalldaempfung in Recheckkanal mit schluckender Wand', (German), Acoustica, vol. 3, 249, (1953).

[4] U. Kurze, 'Schallausbreitung im Kanal mit periodischer Wandstruktur', (German), Acoustica, vol. 21, 74, (1969).

[5] P.M. Morse and U. Ingard, 'Theoretical Acoustics', McGraw-Hill, New York, 1968.

[6] F. Mechel, 'Einfluss der Querunterteilung von Absorbern auf die Schallausbreitung in Kanaelen', (German), Acustica, vol.16, 90, (1965/1966).

[7] U. Ingard and D. Prichmore-Brown, 'Propagation of sound in duct with constrictions', J.A.S.A., vol.23, 689, (1951).

[8] A.G. Heins and H.E. Feshbach, ' The coupling of two acoustical ducts', J. of Math. and Phys., vol. XXVI, 143, (1947).

[9] G.N. Watson, 'A treatise on the theory of Bessel functions', MacMillan, New York, 1944.

[10] F.B. Shenoda, 'Reflexionsarme Abschluss fuer durchstroemte Kanaele', (German), VDI-Gemeinschaftstagung Akoustik und Schwingungstechnik (DAGA), Stuttgart 1972, VDI-Verlag, Berlin, 269, (1972).